Plant Molecular Biology **50:** 587–597, 2002.

Knock-out of *Arabidopsis* metal transporter gene *IRT1* results in iron deficiency accompanied by cell differentiation defects

Rossana Henriques[1,5], Ján Jásik[2,5], Markus Klein[3], Enrico Martinoia[3], Urs Feller[4], Jeff Schell[5], Maria S. Pais[1] and Csaba Koncz[5,*]

[1]*ICAT, Campus da Faculdade de Ciências da Universidade de Lisboa, 1749-016 Lisboa, Portugal;* [2]*Department of Plant Physiology, Comenius University, Mlynska dolina B2, 84 215 Bratislava, Slovakia;* [3]*Université de Neuchâtel, Institut de Botanique, Laboratoire de Physiologie Végétale, Rue Emile Argand 13, CH-2007 Neuchâtel, Switzerland;* [4]*University of Bern, Institute of Plant Sciences, Alterbergrain 21, CH-3013 Bern, Switzerland;* [5]*Max-Planck Institut für Züchtungsforschung, Carl-von-Linné-Weg 10, 50829 Köln, Germany (*author for correspondence, e-mail: koncz@mpiz-koeln.mpg.de)*

Received 28 December 2001; accepted in revised form 25 February 2002

Key words: Arabidopsis, insertion mutagenesis, IRT, metal-transporter, ZIP

Abstract

IRT1 and IRT2 are members of the *Arabidopsis* ZIP metal transporter family that are specifically induced by iron deprivation in roots and act as heterologous suppressors of yeast mutations inhibiting iron and zinc uptake. Although IRT1 and IRT2 are thought to perform redundant functions as root-specific metal transporters, insertional inactivation of the *IRT1* gene alone results in typical symptoms of iron deficiency causing severe leaf chlorosis and lethality in soil. The *irt1* mutation is characterized by specific developmental defects, including a drastic reduction of chloroplast thylakoid stacking into grana and lack of palisade parenchyma differentiation in leaves, reduced number of vascular bundles in stems, and irregular patterns of enlarged endodermal and cortex cells in roots. Pulse labeling with ^{59}Fe through the root system shows that the *irt1* mutation reduces iron accumulation in the shoots. Short-term labeling with ^{65}Zn reveals no alteration in spatial distribution of zinc, but indicates a lower level of zinc accumulation. In comparison to wild-type, the *irt1* mutant responds to iron and zinc deprivation by altered expression of certain zinc and iron transporter genes, which results in the activation of *ZIP1* in shoots, reduction of *ZIP2* transcript levels in roots, and enhanced expression of *IRT2* in roots. These data support the conclusion that IRT1 is an essential metal transporter required for proper development and regulation of iron and zinc homeostasis in *Arabidopsis*.

Abbreviations: IRT, Iron-Regulated Transporter, ZRT, Zinc-Regulated Transporter, ZIP, ZRT, IRT-like Protein

Introduction

Iron limitation is a common form of environmental stress that affects agricultural production worldwide. In many soil types iron is predominantly available as insoluble ferric oxide/hydroxide, which is not readily accessible for uptake by plants. Although a large amount of iron is stored in complex with ferritin within the chloroplasts, this bound iron cannot be mobilized from mature to young leaves (Waldo *et al.*, 1995). Therefore, young leaves become chlorotic during iron limitation due to inhibition of chloroplast biogenesis and chlorophyll biosynthesis. The first signs of leaf chlorosis coincide with morphological alterations in the roots, where root hair formation increases along with thickening of the root cortex (Landsberg, 1994, 1996). In some plant species, but not in *Arabidopsis*, rhizodermal cells differentiate to so-called transfer cells providing a large plasma-membrane surface for enhanced mineral nutrient absorption (Schmidt and Bartels, 1996; Schmidt *et al.*, 2000).

Plants use different strategies to compensate iron limitation (for reviews see Briat *et al.*, 1995; Mori, 1999). Grasses (strategy II plants) release from their roots phytosiderophores that are mugineic acids synthesized from L-methionine through nicotianamine (Shojima *et al.*, 1990; Takahashi *et al.*, 2001). Phytosiderophores are efficient Fe^{2+} and Fe^{3+} chelators that are probably taken up by the roots through membrane transporter homologs of the maize YELLOW STRIPE 1 protein (von Wirén *et al.*, 1999; Curie *et al.*, 2001). Dicotyledonous species (strategy I plants) respond to iron limitation by increased proton extrusion, which leads to acidification of the rhizosphere enhancing the solubilization and reduction of Fe^{3+} (Briat and Lobréaux, 1997; Dell'Orto *et al.*, 2000). Fe^{3+} is reduced by membrane-associated flavocytochrome ferric-chelate reductases and imported into the roots by Fe^{2+}-transporters. Induction of root Fe^{3+}-chelate reductase during iron deprivation is abolished by *frd* mutations in the *Arabidopsis FRO2* gene (Yi and Guerinot, 1996). Although *Arabidopsis* has five *FRO* homologs, one of which (*FRO1*) is also expressed in roots, FRO2 appears to be an enzyme essential for root-specific Fe^{3+}-chelate reduction (Robinson *et al.*, 1999).

Iron deficiency stress leads also to the induction of *i*ron-*r*egulated *t*ransporter genes *IRT1* and *IRT2* in *Arabidopsis* roots. Both IRT1 and IRT2 are capable to suppress the yeast Δ and *zrt1zrt2* mutations that block respectively iron and zinc transport (Eide *et al.*, 1996; Vert *et al.*, 2001). Unlike IRT2, IRT1 can also suppress the *smf1* Δ mutation of a high-affinity manganese transporter and confers cadmium sensitivity when expressed in yeast (Korshunova *et al.*, 1999). Based on transport inhibition studies in yeast, IRT1 is thought to function as broad specificity iron transporter, which also facilitates the transport of zinc and heavy metal cations that accumulate in plants during iron deprivation (Cohen *et al.*, 1998). Site-specific mutagenesis of the predicted metal-binding extracellular loop between transmembrane domains II and III of IRT1 has identified critical residues affecting selective transport of iron, manganese and zinc (Rogers *et al.*, 2000).

Expression of *IRT2* at the root-periphery suggests that IRT1 and IRT2 perform redundant iron and zinc transporter functions (Vert *et al.*, 2001). As zinc transporters, IRT1 and IRT2 appear to act in concert with several zinc-regulated transporters (ZRTs) of the *Arabidopsis* ZIP (ZRT, IRT-like Protein) family (Guerinot, 2000; Mäser *et al.*, 2001). Zinc deficiency induces root-specific expression of ZIP1 and ZIP3, which suppress the *zrt1zrt2*, but not the *fet3fet4*, mutations in yeast (Grotz *et al.*, 1998). ZIP1 and ZIP3 show optimal activity between pH 4.0 and 6.0 when expressed in yeast, whereas ZIP2, a third member of the ZIP family, is inactive below pH 5.0. IRT1, which transports zinc less efficiently than IRT2, is only active below pH 4.2 and requires Fe^{2+} for stimulation of zinc transport (Korshunova *et al.*, 1999).

Despite these characteristic differences, it is difficult to predict whether members of the ZIP family perform overlapping or distinct functions *in vivo*. For example, ZIP4 that is induced by zinc starvation predominantly in leaves cannot transfer zinc and does not complement the *zrt1zrt2* mutations in yeast (Grotz *et al.*, 1998). Functional dissection of 15 members of ZIP transporter gene family identified in the sequenced *Arabidopsis* genome therefore requires the application of reverse genetic approaches that are now facilitated by PCR-screening for insertion mutants (Krysan *et al.*, 1999; Young *et al.*, 2001). The data described here show that a T-DNA insertion mutation in the *IRT1* gene results in typical symptoms of leaf iron deficiency, including chlorosis, inhibition of chloroplast development and lack of palisade parenchyma differentiation. Remarkably, the *irt1* mutant also displays characteristic differentiation defects that affect cell patterns in stems and roots. Seedling lethality caused by the *irt1* knock out indicates that IRT1 functions as essential metal transporter in *Arabidopsis*.

Material and methods

Plant growth conditions and genetic linkage analysis

Arabidopsis thaliana seeds were surface sterilized with 5% calcium hypochlorite solution containing 0.1% Triton X-100 for 15 min, then washed three times with sterile water and dried. Seeds of T-DNA insertion mutants were germinated in MSAR seed medium (Koncz *et al.*, 1994) supplemented with 15 mgl^{-1} hygromycin and grown for 2 weeks in a growth chamber at 23 °C under 200 μEinstein $m^{-2}s^{-1}$ irradiance using 8 hr light and 16 hr dark cycle. To select for iron, zinc, and combined iron and zinc deficiency, M2 and F2 families carrying the *irt1* mutation were germinated on complete MSAR seed medium for 7 days, then transferred on MSAR medium depleted for either iron, or zinc, or both. Following 2 weeks, chlorotic plants carrying the recessive *irt1* mutation in homozygous form were identified and rescued on

MSAR medium for further analysis and planting into soil. Plant growth conditions in soil were as described above, except for using 16 hr light versus 8 hr dark cycle to induce flowering.

Genetic linkage analysis of the T-DNA tagged *irt1* mutation was carried out as described previously for the *ch42/cs* mutation (Koncz *et al.*, 1990), except for that the presence of T-DNA tag at the *irt1* locus was also monitored by PCR amplification in addition to scoring for the yellow phenotype and T-DNA encoded hygromycin resistance marker. M2 and F2 families carrying the *irt1* gene in homozygous form were identified by phenotypic and PCR screening (see below), then subjected to confirmatory Southern DNA hybridizations using *IRT1* cDNA and T-DNA probes as described (Németh *et al.*, 1998). Statistical analysis of segregation data was performed according to Koncz *et al.* (1992).

PCR screening for T-DNA tagged irt1 insertion mutant

A collection of T-DNA insertion mutants was generated by *in planta* transformation of *Arabidopsis thaliana* (Col-0) plants with *Agrobacterium* GV3101 (pMP90RK) harboring the binary vector pPCV6NFHyg (Koncz *et al.*, 1989; Bechtold *et al.*, 1993; Clough and Bent, 1998). Pools of leaf material collected from 100 individual M1 plants were used for preparation of high quality DNA by CsCl-ethidium bromide buoyant density equilibrium gradient centrifugation (Sambrook *et al.*, 1989). DNA samples derived from 100 pools representing 10,000 plants were arranged in a 10 × 10 array to prepare 20 PCR DNA templates by pooling the samples from each row and column. Oligonucleotide primers IRT1-5′ (5′-CACTTCTCATGAAAACAATCTTCCTCGT-3′) and IRT1-3′ (5′-ATCCACATG ATTTCAATTCCGCAAT-3′) for the *IRT1* gene were designed using the PrimerSelect program (DNAStar Inc., Madison, USA) and confirmed to represent unique sequences in the *Arabidopsis* genome by performing BLASTN alignments with the *Arabidopsis* DNA database (http://www.ncbi.nlm.nih.gov). Long-range PCR reactions were carried out with separate combinations of left (5′-CTGGGAATGGCGAAATCAAGGCATC-3′) and right (5′-CAGTCATAGCCGAATAGCCTCTCC A-3′) T-DNA border primers with the IRT1-5′ or IRT1-3′ primers as recommended by the manufacturer (TAKARA Shuzo Co., Shiga, Japan) using a PTC-225 Peltier Thermal Cycler (DNA Engine Systems, MJ Research, Inc., Massachusetts, USA) and a program for 5 min denaturation at 95 °C followed by 35 cycles of 30 sec denaturation at 95 °C and 8.5 min extension at 68 °C, and a final extension step of extension for 10 min at 68 °C. The PCR products were size separated by agarose gel electrophoresis followed by isolation of DNA fragments using a GeneClean kit (BIO 101). The positions of T-DNA ends in the *IRT1* gene were determined by sequencing of PCR-amplified DNA fragments using ABI Prism dye terminator cycle sequencing with the primers IRT1-3′ and IRT1-2-5′ (5′-GGTCTGCAAACGGCATGAACA ATGC-3′). M2 seed progeny from each individual plant represented in the identified DNA pool of 100 M1 plants was germinated and grown for 2 weeks in MSAR agar containing hygromycin. The samples were arranged in a 10×10 array. Five to ten seedlings from each M2 family were used to prepare pools of rows and columns from which DNA was extracted (Rogers and Bendich, 1985) for a repeated PCR screening to identify an M2 family carrying the sequenced T-DNA tagged *irt1* locus.

Comparative histological analysis of wild-type and irt1 *mutant plants*

Wild-type and *irt1* mutant seedlings were either grown for 2 weeks in iron and zinc deficient medium or planted 15 days after germination from iron sufficient medium into soil and grown until onset of flowering. Samples for electron and light microscopy were collected from seedlings grown in sterile cultures, and from identical positions of wild-type and mutant plants of same age grown in soil and were fixed with 4% glutaraldehyde in microtubule stabilizing buffer MTSB (50 mM PIPES, 5 mM $MgSO_4$ and 5 mM EGTA) for 3 h at room temperature. For electron microscopy, the samples were washed with MTSB, then subjected to post-fixing treatment with 1% OsO_4 in MTSB for 1 h, then dehydrated in ethanol at 4 °C and embedded in Spurr-medium (Spurr, 1969). Semi- and ultrathin sections were made with a Reichert Ultracut R (Leica) microtome. Semithin sections of 1 to 2 μm were stained with 1% toluidine blue O in 1% borax and post-stained with 0.1% basic fuchsine. Ultrathin sections were stained with uranylacetate and lead-citrate (Reynolds, 1963) and examined in a Zeiss EM 10C electron microscope. For monitoring the lignification process, hand made stem sections were treated with 1% phloroglucinol in 95% ethanol acidified with HCl.

Pulse labeling of seedlings with ^{59}Fe and ^{65}Zn

Individual wild-type and *irt1* mutant *Arabidopsis thaliana* seedlings were germinated horizontally for one week on the surface of MSAR medium containing 0.4% phytoagar (Duschefa) under short day conditions in order to maintain the root system intact while transferring the seedlings. Subsequently, the plants were transferred for 7 days onto sterile pieces (1.5×1.5 cm^2) of Scrynel NYHC nylon grid (Poly-Labo) layered on the surface MSAR medium free of iron and zinc. For metal uptake assays the seedlings were transferred into Petri-dishes such that the roots hanging down from the grids were submerged into drops of 100 μl buffer A (10 mM MES-KOH [pH 5.7], 1 mM $CaCl_2$) for zinc labeling, and buffer A supplemented with 1 mM sodium ascorbate for iron labeling. The preincubation buffer was removed after 15 min and each seedling was labeled through the root system by addition of 2 μM ^{59}Fe (0.1 μCi/80 pmol, Amersham) in 40 μl Fe-labeling buffer (10 mM MES-KOH [pH 5.7], 1 mM $CaCl_2$, 1 μM $FeSO_4$, and 1 mM sodium ascorbate) for 1h at 25 °C in the light. After removing the Fe-labeling buffer, the roots were rinsed three times with Fe-chase-buffer (10 mM MES-KOH [pH 5.7], 1 mM $CaCl_2$, 1 mM $FeSO_4$, and 10 mM sodium ascorbate), then the grids were transferred into new Petri dishes for washing the roots three times with 50 ml Fe-chase-buffer for 15 min. Pulse-labeling with ^{65}Zn was performed similarly by exposing the roots of each plant to 18 μM ^{65}Zn (0.1 μCi/720 pmol, NEN) in 40 μl Zn-labeling buffer (10 mM MES-KOH [pH 5.7], 1 mM $CaCl_2$, 5 μM $ZnSO_4$) for 1 h at 25 °C in the light. The washing steps were performed as described above in chase-buffer containing 10 mM MES-KOH [pH 5.7] and 2 mM $CaCl_2$. During labeling particular care was taken to prevent the leaves from contacting the labeling buffers. The amount of radioactivity incorporated in dissected roots and shoots was determined by measuring gamma radiation with a 1480 Wizard 3′ Automatic Gamma Counter (Wallac Oy, Finland). To visualize the distribution of incorporated ^{59}Fe, whole seedlings were placed on phosphoimager screens and exposed for 4 weeks. The images were scanned by a STORM860 phosphorimager (Molecular Dynamics) and analyzed using ImageQuant^{TM} software for Macintosh.

Monitoring steady-state transcript levels by reverse transcriptase-PCR

RNA was prepared from wild-type and *irt1* seedlings grown in iron and zinc deficient MSAR medium for 2 weeks using an RNeasy kit (Qiagen, Germany). To perform reverse transcriptase-PCR using an RT-PCR kit (Gibco-BRL), the following cDNA specific primers were used: for IRT1-XbaI (5′-GCCTCTAGAATGAAACAATCTTCCTCGTACTC-3′) and IRT1-BglII (5′-GCCAGATCTAGCCCATTTGGCGATAATCGACAT-3′); IRT2-XbaI (5′-GCCTCTAGAATGGCTACTACCAAGCTCGTCTAC-3′) and IRT2-BglII (5′-GCCAGATCTAGCCCACACGGCGACGACCGA-3′); ZIP1-5′ (5′-GCGGCATTTGGTTTGTTTGTTTGTTAGT-3′) and ZIP1-3′ (5′-TGTCTGAATGTGGATGTTTTTCGGCAAC-3′); ZIP2-5′ (5′-TCCCAAATCATTACAACAGAGAGCAAAG-3′) and ZIP2-3′ (5′-TCTTCCAAAACCCTAAAGTCAACTCTC-3′); ZIP3-5′ (5′-CCTATCCGGTTCATAAAAGCCCTAA-3′) and ZIP3-3′ (5′-TAGAGACATGAGGCCAGCACCAAGA-3′); ZIP4-5′ (5′-TAAACTCTTGTTCCCATGATCTTCGTCA-3′) and ZIP4-3′ (5′-CCCAAATGGCGAGAGCAGACATAAG-3′) and control 18S rRNA primers 18S-5′ (5′-CTGCCAGTAGTCATATGCTTGTC-3′) and 18S-3′ (5′-GTGTAGCGCGCGTGCGGCCC-3′). For cDNA synthesis 2.5 μg total RNA was bound to 4 μl of oligodT cellulose (Boehringer Mannheim) and incubated with SuperScript II reverse transcriptase (Gibco, BRL) at 42 °C for 1 h as recommended by the manufacturer. For PCR amplification 2 μl aliquots from the cDNA synthesis mix were used with IRT and control 18S rRNA primer pairs to perform denaturation at 95 °C for 4 min followed by 35 cycles of denaturation at 95 °C for 1 min, annealing at 68 °C for 1 min and extension at 72 °C for 1 min, and finally by extension at 72 °C for 10 min. For all ZIP primers the conditions for PCR reactions were similar, except that the annealing temperature was 60 °C. The PCR amplified DNA fragments were resolved by agarose gel electrophoresis and the negative images were recorded by a DC120 digital camera using a Kodak Digital Science^{TM} software.

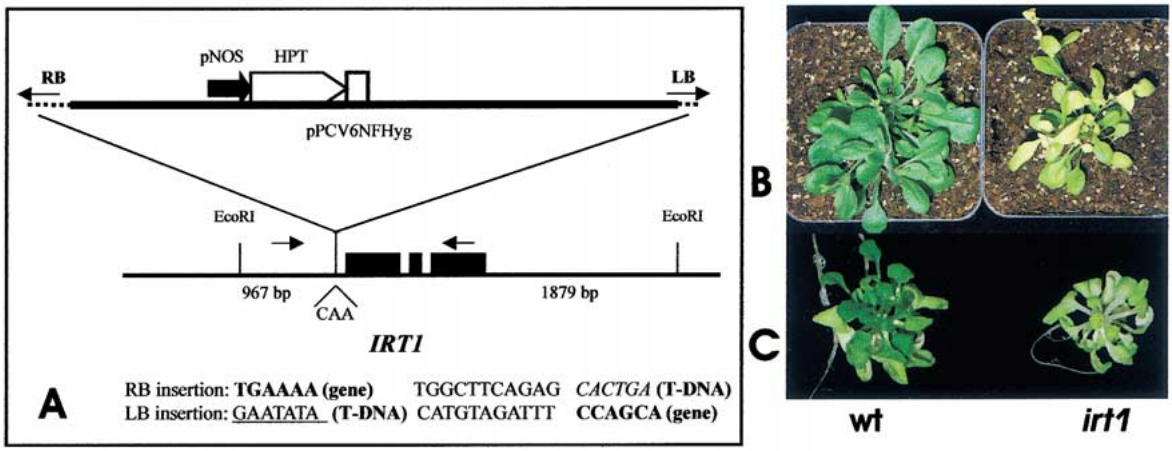

Figure 1. Identification of T-DNA tagged *irt1* locus by PCR-screening of an *Arabidopsis* insertion mutant collection. A. Schematic physical map of tagged *IRT1* gene carrying a single copy insertion of *Agrobacterium* binary vector pPCV6NFHyg T-DNA. A deletion of CAA triplet in the target site is indicated and plant DNA-T-DNA junctions including short filler DNA sequences are shown below the map. Diagnostic *Eco*RI fragments shown in the map were monitored by southern DNA hybridizations in the segregation analysis. Arrows label oligonucleotide primers specific for the *IRT1* gene and T-DNA insert ends. Bold letters mark *IRT1* sequences at the insert junctions. LB and RB, left (underlined) and right (italic) border repeats of the T-DNA; HPT, hygromycin resistance gene; and pNOS, nopaline synthase promoter (Koncz *et al.*, 1989). B. Wild-type (left) and *irt1* mutant (right) plants were grown in iron sufficient MSAR medium, then planted into soil and grown for 7 days. C. Wild-type (left) and *irt1* mutant (right) seedlings grown in iron and zinc deficient MSAR medium *in vitro*.

Results

Isolation of irt1 *T-DNA insertion mutant*

To perform a PCR screening for T-DNA insertion in the *IRT1* gene, an M1 mutant population of 10,000 *Arabidopsis* plants was generated by *Agrobacterium*-mediated *in planta* transformation using the T-DNA vector pPCV6NFHyg (Koncz *et al.*, 1989). The collection was arranged in a 10 × 10 array, in which each sample represented DNA from 100 M1 plants. The pooled rows and columns from the array yielded 20 PCR DNA templates, each corresponding to 1,000 plants. Oligonucleotide primers specific for the 5′ or 3′ ends of the *IRT1* gene were combined with primers annealing to either the left or the right end of pPCV6NFHyg T-DNA to perform 4 × 20 long-range PCR reactions. Electrophoretic detection of DNA fragments carrying the left and right T-DNA-plant DNA insert junctions identified a row/column intersection corresponding to a pool of 100 plants that contained a T-DNA tagged *irt1* gene. A second turn of PCR screen, performed with a 10 × 10 array of DNA templates, derived from individual plants of this pool led to the identification of a single mutant line carrying the *irt1* mutation in hemizygous form. Nucleotide sequencing of T-DNA insert junctions amplified by PCR from the M2 progeny of identified mutant line revealed a single copy T-DNA insertion 133 bp upstream of the predicted ATG codon of *IRT1* coding region on chromosome 4 (Genbank gi‖15233324). The T-DNA insertion generated a target-site deletion of 3 bp and short stretches of filler DNA at both left and right T-DNA border junctions (Figure 1A). The insertion retained 17 bp from the left 25 bp border sequence, whereas a deletion of 2 bp downstream of the canonical border sequence was detected at the right T-DNA end.

Inspection of 15 M2 families by southern DNA hybridization using T-DNA and *IRT1* cDNA probes (data not shown) indicated that the original M1 mutant line carried one additional T-DNA tagged chromosomal locus, which segregated independently of the *irt1* mutation. M2 individuals harboring the *irt1* mutation were crossed with wild-type to obtain segregating F2 families by self-pollination of F1 hybrids. As seen in the M2 families, all F2 families carrying the T-DNA tagged *irt1* locus segregated in iron and zinc deficient medium and in soil green and yellow plants at a 3:1 ratio (Figure 1B and C). The segregation analysis indicated about 25% reduction in the transmission of recessive *irt1* mutation (n=4, homogeneity = 3.175, p = 0.35; Koncz *et al.*, 1992). After transferring into iron supplemented medium, all yellow mutants turned green, but when planted subsequently into soil showed gradual bleaching and retardation of development, and ultimately died producing little or no seed. Molecular

analysis of F2 progeny showed that all yellow plants carried the T-DNA-tagged *irt1* locus in homozygous form, whereas no F2 family lacking the *irt1* mutation segregated yellow progeny. The genetic linkage analysis thus indicated that the observed phenotype was caused by knock-out of the *IRT1* gene and not by another insertion event or a linked, but untagged, mutation.

Cell differentiation defects in the irt1 *mutant*

Chlorosis of leaves is a classical symptom of iron deficiency resulting in inhibition of chlorophyll biosynthesis and chloroplast development (Briat and Lobréaux, 1997). When grown in iron and zinc deficient medium with sufficient amount of sucrose as carbon source for 2 weeks, the *irt1* mutant turned fully chlorotic, whereas control wild-type plants showed chlorosis only in older rosette leaves (Figure 1C). When planted into soil from iron-supplemented medium, the *irt1* mutant developed typical signs of iron deficiency within days by displaying progressive bleaching of inflorescence stems, fruits, cauline and rosette leaves (Figure 1B). The subepidermal layer of palisade parenchyma cells characteristic for wild-type leaves was not properly differentiated in *irt1* mutant leaves (Figure 2A). As observed in iron-deficient leaves, chloroplasts in *irt1* parenchyma cells displayed a drastic reduction of thylakoid stacking into grana and contained less and smaller starch grains than chloroplasts of wild-type plants grown under identical conditions (Figure 2B). Retarded development of *irt1* mutant was also accompanied by changes in proper differentiation of vascular tissue in stems. In contrast to a regular octameric arrangement detectable in wild-type plants, the *irt1* mutant contained only 5 to 6 unequally developed vascular bundles in the primary stem (Figure 3B). The *irt1* mutant also showed an overall reduction of secondary stem thickening and absence of secondary xylem and phloem in some vascular bundles. Remarkably, the well-characterized pattern of cell files detected in roots of wild-type plants could barely be recognized in the *irt1* mutant, which displayed an irregular number and altered pattern of swollen root endodermal and cortex cells (Figure 3A).

The irt1 *mutation causes iron depletion in the shoots*

To determine the effect of *irt1* mutation on iron transport, short-term pulse-labeling experiments were performed with ^{59}Fe. Wild-type and *irt1* mutant plants grown on grids by submerging the roots into iron and zinc deficient liquid medium were labeled for 1 h through the root system with ^{59}Fe, which was reduced to ferrous cation by 1mM sodium ascorbate in the labeling buffer. To reduce nonspecific binding of ^{59}Fe to a minimum, the roots were extensively washed with a buffer containing 1mM $FeSO_4$ and 10 mM sodium ascorbate after labeling. Harvesting the roots in bulk from a pool of plants and calculation of the amount of incorporated ^{59}Fe using a standard method (Cohen *et al.*, 1998) resulted in large variations due to unequal drying of roots before measuring their wet-weight. To avoid this experimental bias, the distribution of ^{59}Fe was determined by measuring the incorporated radioactivity in excised shoots and roots of large number of individual plants. Statistical evaluation of data (Figure 4B) indicated that the total amount of ^{59}Fe incorporated into wild-type plants was on an average 127.7±60.7 fmol/plant showing a nearly equal distribution between roots (54.2%) and shoots (45.8%). By contrast, the *irt1* mutant accumulated significantly less ^{59}Fe (81.45±29.35 fmol/plant) and displayed about 2-fold less accumulation of ^{59}Fe in shoots (29.3%) as compared to roots (70.6%). In comparison to wild-type, the total amount of ^{59}Fe incorporated into shoots during 1 h of pulse labeling was 2.5-fold less in the *irt1* mutant. Visualization of pulse-labeled seedlings by phosphoimaging detected thus somewhat weaker labeling of roots, but clearly lower level of radioactivity in shoots of the *irt1* mutant as compared to ^{59}Fe-labeling of wild-type seedlings (Figure 4A). These data indicated that the *irt1* mutation did not abolish the uptake of iron through the root system, but caused significant iron depletion in the shoots. The fact, that a residual iron uptake capacity was maintained, probably due to the activity of second root-specific iron transporter IRT2, was also suggested by the observation that chlorotic *irt1* seedlings were capable of re-greening when transferred from iron deficient to iron-containing medium. However, this residual iron uptake capacity was clearly insufficient for survival of the *irt1* mutant in soil indicating that IRT1 is an essential iron transporter in *Arabidopsis*.

The effect of irt1 *mutation on zinc regulation*

When expressed in yeast, IRT1 was observed to catalyze Fe^{2+}-facilitated zinc transport at low pH (Korshunova *et al.*, 1999). Nonetheless, similar pulse-labeling experiments with ^{65}Zn under combined iron and zinc depletion failed to reveal any significant difference between ratios of zinc accumulation in

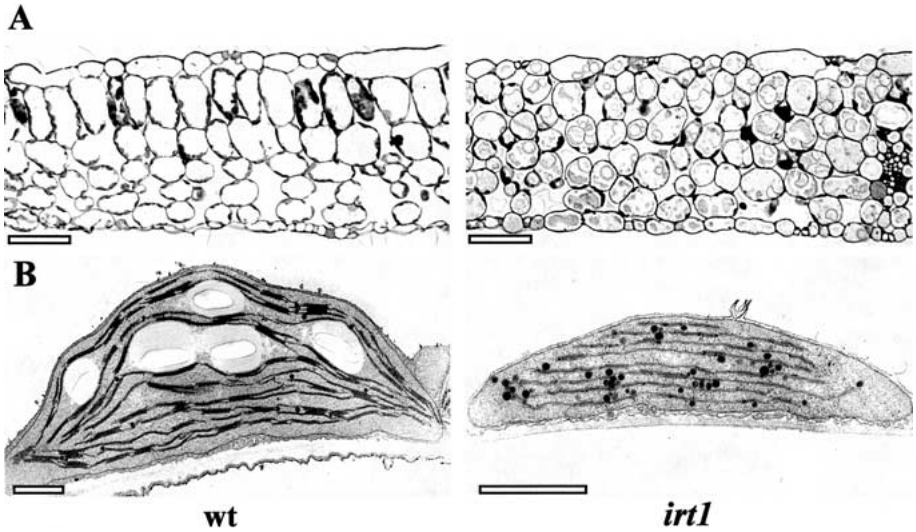

Figure 2. A. Transversal section of leaves from wild-type (left) and *irt1* mutant (right) plants grown in soil. The subepidermal layer of palisade parenchyma cells present in the wild-type is not properly differentiated in the *irt1* mutant. Bars: 50 μm. B. In comparison to chloroplasts in wild-type (left) leaves, chloroplasts in the *irt1* mutant (right) develop reduced thylakoid system and contain maximum 2 to 3 thylakoids per grana. Bars in the electronmicrographs: 0.5 μm.

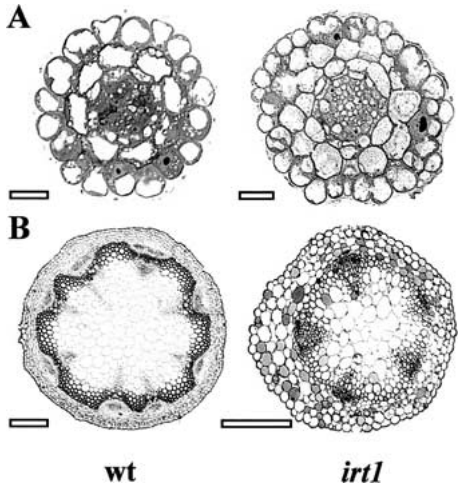

Figure 3. A. Transversal sections taken at the beginning of elongation zones from wild-type (left) and *irt1* mutant (right) roots show more loosely arranged and enlarged cells in the endodermal and cortex layers of mutant roots. Bar: 25 μm. B. Stem cross-sections from wild-type (left) and *irt1* mutant (right) plants indicate a reduction in the number of vascular bundles from regular 8 to 5, showing unequal development and irregular arrangement. Bar: 0.5 mm.

shoots and roots of wild-type and *irt1* mutant seedlings (Figure 4C). However, the amounts of ^{65}Zn incorporated into *irt1* shoots (177.43±94.9 fmol/plant) and roots (412.12±271.7 fmol/plant) were respectively 2.02±0.47 and in 2.50±0.46 times lower than in wild-type indicating that the *irt1* mutation caused a significant zinc depletion without affecting zinc distribution.

Zinc deficiency was previously shown to result in root-specific induction of transcription of *ZIP1* and *ZIP3* zinc transporter genes (Grotz *et al.*, 1998), whereas iron deficiency was found to similarly activate the *IRT1* and *IRT2* genes in *Arabidopsis* roots. As reported for iron and zinc deficiency separately (Eide *et al.*, 1996; Grotz *et al.*, 1998; Vert *et al.*, 2001), determination of steady-state transcript levels by RT-PCR amplification showed that the *IRT1*, *IRT2*, *ZIP1* and *ZIP3* genes were also induced in roots of wild-type plants under combined Fe and Zn deficiency conditions used in our pulse-labeling experiments (Figure 5). *ZIP2*, the transcript of which could not be detected previously (Eide *et al.*, 1996), also displayed root-specific expression, whereas the *ZIP4* transcript was observed, as expected, at a much higher level in shoots than in roots. The *irt1* mutation did not alter the *ZIP3* and *ZIP4* mRNA levels, but caused a significant reduction of *ZIP2* transcript level in roots. By contrast, *ZIP1* displayed an unexpected activation in shoots correlating with a decreased zinc accumulation in the *irt1* mutant. Furthermore, significantly increased steady-state *IRT2* transcript levels were observed in *irt1* roots suggesting that a compensatory mechanism may exist, which responds by enhanced induction of the *IRT2* iron transporter gene to elevated iron deficiency resulting from inactivation of the IRT1 function.

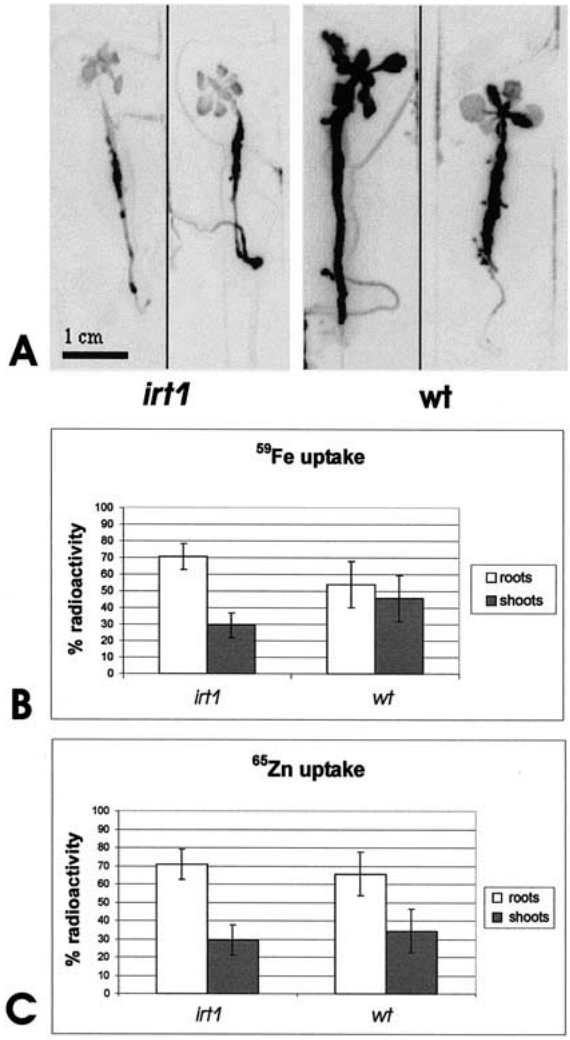

Figure 4. Pulse-labeling of wild-type and *irt1* mutant seedlings with ^{59}Fe and ^{65}Zn. A. Detection of ^{59}Fe accumulation in *irt1* mutant (left) and wild-type (right) seedlings after 1 h of labeling by phosphoimaging. B. Distribution of ^{59}Fe in shoots and roots of *irt1* and wild-type seedlings. C. Distribution of ^{65}Zn in shoots and roots of *irt1* and wild-type seedlings. Columns indicate the means, whereas bars show standard deviations. The shoot-to-root ratios of ^{59}Fe and ^{65}Zn incorporation were determined in four independent pulse-labeling experiments using 10 to 20 individual wild-type and *irt1* seedlings in each assay.

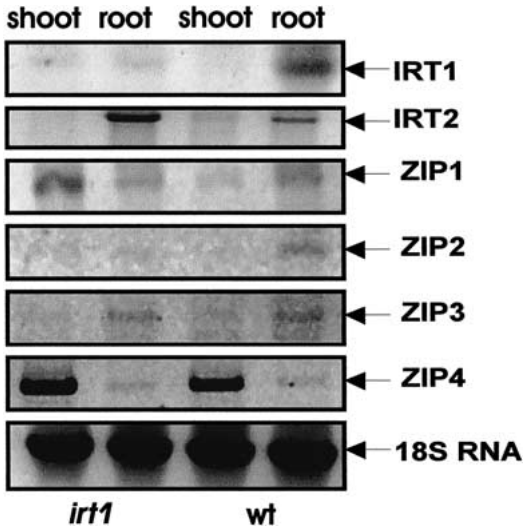

Figure 5. RT-PCR analysis of steady-state transcript levels of *IRT* and *ZIP* transporter genes in wild-type and *irt1* mutant seedlings grown for 2 weeks in iron and zinc deficient medium. The PCR amplified cDNAs were size separated on 0.8% agarose gels to electronically record negative images of ethidium-bromide stained bands.

Discussion

IRT1, the founding member of ZIP transporter family, was identified by a powerful suppressor screen based on the complementation of yeast *fet3* multicopper oxidase and *fet4* Fe(II)-transporter mutations that block high and low affinity iron transport, respectively (Askwith *et al.*, 1994; Dix *et al.*, 1994; Eide *et al.*, 1996). IRT1 was also found to suppress the *zrt1zrt2* mutations of high and low-affinity zinc transporters and the *smf1*Δ mutation of a high-affinity Nramp manganese transporter, as well as to increase cadmium sensitivity, when expressed in yeast (Korshunova *et al.*, 1999; Rogers *et al.*, 2000). Nonetheless, IRT1 turned out to differ both structurally and functionally from these yeast transporter proteins, but shows homology to numerous putative membrane proteins in eukaryotes, including predicted products of 15 *ZIP* genes in the sequenced *Arabidopsis* genome (Guerinot, 2000; Mäser *et al.*, 2001). Characterization of other members of ZIP family indicated that IRT2, a close homolog of IRT1, facilitates iron and zinc uptake, whereas ZIP1, ZIP2 and ZIP3 mediate only zinc transport in yeast. *IRT1* and *IRT2* are induced by iron depletion, whereas *ZIP1*, *ZIP2* and *ZIP3* are activated by zinc deficiency specifically in *Arabidopsis* roots (Eide *et al.*, 1996; Grotz *et al.*, 1998; Vert *et al.*, 2001). By contrast ZIP4, carrying a putative chloroplast signal peptide, was suggested to function as leaf specific zinc-regulated transporter (Grotz *et al.*, 1998). In addition to the ZIP family, however, 3 members of the *Arabidopsis* NRAMP (natural-resistance-associated macrophage protein) family were also identified to respond to iron depletion and to mediate iron and cadmium uptake (Curie *et al.*, 2000; Thomine *et al.*, 2000). Recent finding of homologs of maize

YS1 (*yellow strip 1*) gene in *Arabidopsis* suggests that even further transporters are implicated in the control of iron homeostasis in plants (Curie *et al.*, 2001).

This high redundancy raises the logical question whether reverse genetics, producing single recessive or dominant gene mutations, would be helpful in the dissection of physiological functions of individual plant metal transporters. The knock-out of IRT1 function described above provides an encouraging answer suggesting that quantitative differences in the contribution of individual metal transporters, as well as differences in their spatial and temporal regulation, may result in characteristic phenotypes of individual transporter mutants. Thus, our data show that inactivation of *IRT1* results in shoot iron deficiency leading to severe chlorosis and lethality. However, it is likely that the reduction of zinc uptake in the *irt1* mutant contributes to the phenotype, as the *irt1* mutant shows also bleaching in zinc-depleted iron-sufficient medium (unpublished). Characteristic changes in the differentiation of specific cell layers in leaf, stem and root may thus reflect consequences of a combined iron and zinc deficiency in the *irt1* mutant. Due to functional redundancy of iron and zinc transporters, the *irt1* knock-out does not completely abolish iron and zinc uptake by the roots, thus the otherwise unviable chlorotic *irt1* mutant can be rescued to wild-type by providing external iron and zinc. However, the dramatic phenotype of the *irt1* mutant demonstrates that the contribution of IRT1 to the maintenance of iron and zinc homeostasis is essential, despite a redundancy of root-specific iron and zinc transporters. Thus, neither IRT2 nor other IRT-like and ZIP genes listed in the *Arabidopsis* genome database seem to be able to compensate for the reduction of iron and zinc accumulation caused by the loss of IRT1 function, although the expression of the *IRT2* gene is considerably higher in *irt1* roots than in wild-type. To classify IRT1, e.g. based on a comparison to IRT2 in yeast, as high-affinity iron transporter is nevertheless premature as detailed biochemical characterization of these proteins is further awaited in *Arabidopsis*. This should also help to define the quantitative contribution of IRT1 and IRT2 to iron accumulation in the roots and further iron transport into the shoots. Our pulse-labeling experiments with ^{59}Fe seem to contradict the data of Yi and Guerinot (1996), who found very little iron accumulation in shoots within the first hour of ^{55}Fe trace labeling. As in our case, however, similar quantities of ^{55}Fe were detected upon 48 h uptake in shoots and roots of wild-type plants. More importantly, Yi and Guerinot (1996) demonstrated that *frd1* mutations of the *Arabidopsis FRO2* Fe^{3+}-chelate reductase gene significantly reduce iron uptake and transport by the roots indicating that FRO2 is obligatorily required to satisfy Fe^{2+}-specificity of root iron transporters. How iron and zinc are transported from the epidermis via the cortex and endodermis of roots through the vascular tissues into the shoots is an intriguing question. Recently, the expression of *IRT2* has been localized to the root epidermal (i.e. rhizodermal) layer by monitoring the activity of a promoter-GUS reporter gene fusion (Vert *et al.*, 2001). Nonetheless, to understand how IRT1 and IRT2 regulate the transport of iron and zinc between root cell layers and from roots to shoots, further studies of IRT1 expression pattern and stability of IRT1 and IRT2 transporters in reciprocal knock-out mutants are required.

An intriguing aspect of iron and zinc uptake studies is the regulation of gene expression under deficiency stress conditions. Recent transcript profiling experiments using microarrays of *Arabidopsis* cDNAs indicate that a battery of genes involved in anaerobic respiration in roots, as well as in gluconeogenesis, starch degradation, phloem loading, tricarboxylic acid cycle and oxidative pentose phosphate pathway in shoots, are induced in response to iron deficiency stress (Thimm *et al.*, 2001). Analogous transcript profiling experiments in yeast have identified 46 genes controlled by the transcription factor ZAP1 that binds to zinc-responsive elements of promoters regulated by zinc deprivation (Lyons *et al.*, 2000). Yeast Aft1 and Aft2 were similarly defined as transcription factors required for resistance to oxidative stress and regulation of genes induced by iron deficiency (Blaiseau *et al.*, 2001). The availability of *irt1* knock out mutation affecting the regulation of IRT2, ZIP1 and ZIP2 target genes offers now a suitable system for identification of iron and zinc responsive "regulons" in *Arabidopsis*. In addition, restoration of deficient phenotype to wild-type by externally added iron and zinc provides a useful internal control to study how iron deficiency induces oxidative stress leading to progressive chlorosis and ultimate death in the *irt1* mutant.

Acknowledgements

The authors thank Mrs A. Lossow and S. Schäfer for their excellent technical assistance, and Drs G. Molnár, A. Mouradov and G. Coupland for their critical comments on the manuscript. This work was

supported by grants from the European Commission (QLRT-2000-01871) and Deutsche Forschungsgemeinschaft (KO1483/3-1) for C.K. and from the Fundação para a Ciência e Tecnologia – Ministério da Ciência e Tecnologia (BD 11502/97) for R.H.

References

Askwith, C., Eide, D., Van Ho, A., Bernard, P.S., Li, L., Davis-Kaplan, S., Sipe, D.M. and Kaplan, J. 1994. The *FET3* gene of *S. cerevisiae* encodes a multicopper oxidase required for ferrous iron uptake. Cell 76: 403–410.

Bechtold, N., Ellis, J. and Pelletier, G. 1993. *In planta Agrobacterium* mediated gene transfer by infiltration of adult *Arabidopsis thaliana* plants. C. R. Acad. Sci. Paris, Life Sciences, 316: 1194–1199.

Blaiseau, P.L., Lesuisse. E. and Camadro, J.M. 2001. Aft2p, a novel iron-regulated transcription activator that modulates, with Aft1p, intracellular iron use and resistance to oxidative stress in yeast. J. Biol. Chem. 276: 34221–34226.

Briat, J.-F., Fobis-Loisy, I., Grignon, N., Lobréaux. S., Pascal, N., Savino, G., Thoiron, S., von Wirén, N. and Van Wuytswinkel, O. 1995. Cellular and molecular aspects of iron metabolism in plants. Biol. Cell 84: 69–81.

Briat, J.-F. and Lobréaux, S. 1997. Iron transport and storage in plants. Trends Plant Sci. 2: 187–193.

Clough, S.J. and Bent, A.F. 1998. Floral dip: a simplified method for *Agrobacterium*-mediated transformation of *Arabidopsis thaliana*. Plant J. 16: 735–743.

Cohen, C.K., Fox, T.C., Garvin, D.F. and Kochian, L.V. 1998. The role of iron-deficiency stress responses in stimulating heavy-metal transport in plants. Plant Physiol. 116: 1063–1072.

Curie, C., Alonso, J.M., Le Jean, M., Ecker, J.R. and Briat, J.F. 2000. Involvement of NRAMP1 from *Arabidopsis thaliana* in iron transport. Biochem J. 347: 749–755.

Curie, C., Panaviene, Z., Loulergue, C., Dellaporta, S.L., Briat, J.-F. and Walker, E.L. 2001. Maize *yellow stripe 1* encodes a membrane protein directly involved in Fe(III) uptake. Nature 409: 346–349.

Dell'Orto, M., Santi, S., De Nisi, P., Cesco, S., Varanini, Z., Zocchi, G. and Pinton, R. 2000. Development of Fe-deficiency responses in cucumber (*Cucumis sativus* L.) roots: involvement of plasma membrane H^+-ATPase activity. J. Exp. Bot. 51: 695–701.

Dix, D.R., Bridgham, J.T., Broderius, M.A., Byersdorfer, C.A. and Eide, D.J. 1994. The *FET4* gene encodes the low affinity Fe(II) transport protein of *Saccharomyces cerevisiae*. J. Biol. Chem. 269: 26092–26099.

Eide, D., Broderius, M., Fett, J. and Guerinot, M.L. 1996. A novel iron-regulated metal transporter from plants identified by functional expression in yeast. Proc. Natl. Acad. Sci. USA 93: 5624.5628.

Grotz, N., Fox, T., Connolly, E., Park, W., Guerinot, M.L. and Eide, D. 1998. Identification of a family of zinc transporter genes from *Arabidopsis* that respond to zinc deficiency. Proc. Natl. Acad. Sci. USA 95: 7220–7224.

Guerinot, M.L. 2000. The ZIP family of metal transporters. Biochem. Biophys. Acta 1465: 190–198.

Koncz, C., Martini, N., Mayerhofer, N., Koncz-Kálmán, Z., Körber, H., Rédei, G.P. and Schell, J. 1989. High-frequency T-DNA-mediated gene tagging in plants. Proc. Natl. Acad. Sci. USA 86: 8467–8471.

Koncz, C., Mayerhofer, R., Koncz-Kálmán, Z., Nawrath, C., Reiss, B., Rédei, G.P. and Schell, J. 1990. Isolation of a gene encoding a novel chloroplast protein by T-DNA tagging in *Arabidopsis thaliana*. EMBO J. 9: 1337–1346.

Koncz, C., Chua, N.-H. and Schell, J. 1992. Methods in *Arabidopsis* Research. World Scientific, Singapore

Koncz, C., Martini, N., Szabados, L., Hrouda, M., Bachmair, A. and Schell, J. 1994. Specialized vectors for gene tagging and expression studies. In Gelvin, S.B. and Schilperoort, R.A. (Eds) Plant Molecular Biology Manual, Kluwer Academic Press, Dordrecht, B2: pp. 1–22.

Korshunova, Y.O., Eide, D. Clark, G.W., Guerinot, M.L. and Pakrasi, H.B. 1999. The IRT1 protein from *Arabidopsis thaliana* is a metal transporter with a broad substrate specificity. Plant Mol. Biol. 40: 37–44.

Krysan, P.J., Young, J.C. and Sussman, M.R. (1999) T-DNA as an insertional mutagen in *Arabidopsis*. Plant Cell 12: 2283–2290.

Landsberg, E.C. 1994. Transfer cell formation in sugar beet roots induced by latent Fe deficiency. Plant Soil 165: 197–205.

Landsberg, E.C. 1996. Hormonal regulation of iron-stress response in sunflower roots: a morphological and cytological investigation. Protoplasma 194: 60–80.

Lyons, T.J., Gasch, A.P., Gaither, A.L., Botstein, D., Brown, P.O. and Eide, D.J. 2000. Genome-wide characterization of the Zap1p zinc-responsive regulon in yeast. Proc. Natl. Acad. Sci. USA 97: 7957–7962.

Mäser, P., Thomine, S., Schroeder, J.I., Ward, J.M., Hirschi, K., Sze, H., Talke, I.N., Amtmann, A., Maathuis, F.J.M., Sanders, D., Harper, J.F., Tchieu, J., Gribskov, M., Persans, M.W., Salt, D.E., Kim, S.A. and Guerinot, M.L. 2001. Phylogenetic relationships within cation transporter families of *Arabidopsis*. Plant Physiol. 126: 1646–1667.

Mori, S. 1999. Iron acquisition in plants. Curr. Opin. Plant Biol. 2: 250–253.

Németh, K., Salchert, K., Putnoky, P., Bhalerao, R., Koncz-Kálmán, Z., Stankovic-Stangeland, B., Bakó, L., Mathur, J., Ökrész, L., Stabel, S., Geigenberger, P., Stitt, M., Rédei, G.P., Schell, J. and Koncz, C. 1998. Control of glucose and hormone responses by PRL1, a nuclear WD-protein, in *Arabidopsis*. Genes Devel. 12: 3059–3073.

Reynolds, E.S. 1963. The use of lead citrate at high pH as an electronopaque stain in electron microscopy. J. Cell. Biol. 17: 208–212.

Robinson, N.J., Procter, C.M., Connolly, E.L. and Guerinot, M.L. 1999. A ferric-chelate reductase for iron uptake from soils. Nature 397: 694–697.

Rogers, S.O. and Bendich, A.J., 1985. Extraction of DNA from milligram amounts of fresh, herbarium and mummified plant tissues. Plant Mol. Biol. 5: 69–76.

Rogers, E.E., Eide, D.J. and Guerinot, M.L. 2000. Altered selectivity in an *Arabidopsis* metal transporter. Proc. Natl. Acad. Sci. USA 97: 12356–12360.

Sambrook, J., Fritsch, E.F. and Maniatis, T. 1989. Molecular Cloning: A Laboratory Manual. Cold Spring Harbor Laboratory Press, Cold Spring Harbor, N.Y.

Schmidt, W. and Bartels, M. 1996. Formation of root epidermal transfer cells in *Plantago*. Plant Physiol. 110: 217–225.

Schmidt, W., Tittel, J. and Schikora, A. 2000. Role of hormones in the induction of iron deficiency responses in *Arabidopsis* roots. Plant Physiol. 122: 1109–1118.

Shojima, S., Nishizawa, N.K., Fushiya, S., Nozoe, S., Irifune, T. and Mori, S. 1990. Biosynthesis of phytosiderophores. *In vitro* biosynthesis of 2′-deoxymugineic acid from L-methionine and nicotianamine. Plant Physiol. 93: 1497–1503.

Spurr, A.R. 1969. A low-viscosity epoxy resin embedding medium for electron microscopy. J. Ultrastruc. Res. 26: 31–43.

Takahashi, M., Nakanishi, H., Kawasaki, S., Nishizawa, N.K. and Mori, S. 2001. Enhanced tolerance of rice to low iron availability in alkaline soils using barley nicotianamine aminotransferase genes. Nature Biotech. 19: 466–469.

Thimm, O., Essigmann, B., Kloska, S., Altmann, T. and Buckhout, T.J. 2001. Response of *Arabidopsis* to iron deficiency stress as revealed by microarray analysis. Plant Physiol. 127: 1030–1043.

Thomine, S., Wang, R., Ward, J.M., Crawford, N.M. and Schroeder, J.I. 2000. Cadmium and iron transport by members of a plant metal transporter family in *Arabidopsis* with homology to *Nramp* genes. Proc. Natl. Acad. Sci. USA 97: 4991–4996.

Vert, G., Briat, J.-F. and Curie, C. 2001. *Arabidopsis IRT2* gene encodes a root-periphery iron transporter. Plant J. 26: 181–189.

Von Wirén, N., Klair, S., Bansal, S., Briat, J.-F., Khodr, H., Shioiri, T., Leigh, R.A. and Hider, R.C. 1999. Nicotianamine chelates both Fe III and Fe II. Implications for metal transport in plants. Plant Physiol. 119: 1107–1114.

Waldo, G.S., Wright, E., Whang, Z.H., Briat, J.F., Theil, E.C. and Sayers, D.E. 1995. Formation of the ferritin iron mineral occurs in plastids. Plant Physiol. 109: 797–802.

Yi, Y. and Guerinot, M.L. 1996. Genetic evidence that induction of root Fe(III) chelate reductase activity is necessary for iron uptake under iron deficiency. Plant J. 10: 835–844.

Young, J.C., Krysan, P.J. and Sussman, M.R. 2001. Efficient screening of *Arabidopsis* T-DNA insertion lines using degenerate primers. Plant Physiol. 125: 513–518.